Received: 22 December 2020 | Accepted: 9 June 2021

DOI: 10.1111/gcb.15754

Global Change Biology WILEY

PRIMARY RESEARCH ARTICLE

Long-term geothermal warming reduced stocks of carbon but not nitrogen in a subarctic forest soil

Tino Peplau[1] | Julia Schroeder[1] | Edward Gregorich[2] | Christopher Poeplau[1]

[1]Thünen Institute of Climate-Smart Agriculture, Braunschweig, Germany

[2]Ottawa Research and Development Centre, Central Experimental Farm, Agriculture and Agri-Food Canada, Ottawa, ON, Canada

Correspondence
Christopher Poeplau, Thünen Institute of Climate-Smart Agriculture, Bundesallee 65, Braunschweig, Germany.
Email: christopher.poeplau@thuenen.de

Funding information
Science & Technology Branch of Agriculture & Agri-Food Canada, Grant/Award Number: J-001756; Deutsche Forschungsgemeinschaft, Grant/Award Number: 401106790

Abstract

Global warming is accelerating the decomposition of soil organic matter (SOM). When predicting the net SOM dynamics in response to warming, there are considerable uncertainties owing to experimental limitations. Long-term in situ whole-profile soil warming studies are particularly rare. This study used a long-term, naturally occurring geothermal gradient in Yukon, Canada, to investigate the warming effects on SOM in a forest ecosystem. Soils were sampled along this thermosequence which exhibited warming of up to 7.7°C; samples were collected to a depth of 80 cm and analysed for soil organic carbon (SOC) and nitrogen (N) content, and estimates made of SOC stock and fractions. Potential litter decomposition rates as a function of soil temperature and depth were observed for a 1-year period using buried teabags and temperature loggers. The SOC in the topsoil (0–20 cm) and subsoil (20–80 cm) responded similar to warming. A negative relationship was found between soil temperature and whole-profile SOC stocks, with a total loss of 27% between the warmest and reference plots, and a relative loss of 3%°C^{-1}. SOC losses were restricted to the particulate organic matter (POM) and dissolved organic carbon (DOC) fractions with net whole-profile depletions. Losses in POM-C accounted for the largest share of the total SOC losses. In contrast to SOC, N was not lost from the soil as a result of warming, but was redistributed with a relatively large accumulation in the silt and clay fraction (+40%). This suggests an immobilization of N by microbes building up in mineral-associated organic matter. These results confirm that soil warming accelerates SOC turnover throughout the profile and C is lost in both the topsoil and subsoil. Since N stocks remained constant with warming, SOM stoichiometry changed considerably and this in turn could affect C cycling through changes in microbial metabolism.

KEYWORDS
Canada, fractionation, soil organic matter, soil warming, Takhini hot springs, teabags, thermosequence, whole-profile

1 | INTRODUCTION

Climate change and the associated rise in temperatures leads to warming of soils (Heimann & Reichstein, 2008). Microbial activity, and thus decomposition of soil organic matter (SOM), is stimulated by warming and is likely to turn soils into a net source of carbon dioxide (CO_2), inducing a climate-carbon cycle feedback loop (Heimann & Reichstein, 2008). The largest temperature increases

are expected in high latitudes (IPCC, 2013, 2019), where soils store the most (FAO and ITPS, 2017) and oldest SOM (Shi et al., 2020). Therefore, boreal biomes are considered to be of major importance for the global C cycle and play an import role in climate change feedbacks (Carey et al., 2016). The effect of rising air temperatures and other global change drivers on ecosystems has been extensively studied in the last four decades (Song et al., 2019). However, predictions about the responses of SOM to warming are difficult and uncertain, due to a lack of long-term field warming experiments, investigating whole-soil profile interactions between soil warming and the C and nitrogen (N) cycles. Most in situ warming studies have a time span of less than a decade, and usually of just 1–3 years (Eliasson et al., 2005; Hicks Pries et al., 2017; Ineson et al., 1998; Li et al., 2018; Luo et al., 2001; Nottingham et al., 2020). Furthermore, also laboratory incubation experiments have short time spans of observations (Aaltonen et al., 2019; Conen et al., 2006; Dutta et al., 2006; Karhu et al., 2010), while climate change is a slow, gradual process with many interactions between ecosystem components that require longer observations. Depending on warming intensity and the soil parameters being investigated, abrupt soil warming can lead to overshoot reactions or relatively fast equilibration (Walker et al., 2020). Melillo et al. (2017) reported strong temporal trends in SOC losses over 26 years of soil warming with different stages of SOC loss and build-up, resulting in a non-linear relationship between warming duration and SOC loss. Short-term experiments might thus risk overestimating warming effects when linearly extrapolated to longer timescales (Crowther et al., 2016); they certainly fail to predict how strongly, depending on warming intensity, ecosystem processes will change before a new steady state might be reached (Walker et al., 2020). However, understanding the new baseline of specific parameters after long-term warming is crucial for an overall quantitative understanding of warming effects on ecosystem processes.

Even though subsoil (usually defined as the soil below the A-horizon or the soil below the main rooting zone) stores around 50% of total SOC stocks (Hicks Pries et al., 2017; Koarashi et al., 2012; Rumpel & Kögel-Knabner, 2011; Wordell-Dietrich et al., 2017), most warming experiments have focused on the topsoil. Few studies have evaluated whole-profile warming (e.g. Nottingham et al., 2020: 120 cm and Hicks Pries et al., 2017: 100 cm). In subsoils, the abiotic conditions, the availability of fresh substrates, SOM composition and the size and structure of the microbial community are very different from those in topsoils (Fierer et al., 2003; Rumpel & Kögel-Knabner, 2011). It is therefore reasonable to expect that the response of subsoils to warming would be different from that of topsoils.

The fate of N under long-term warming has not been thoroughly characterized in studies evaluating the response of SOM to warming. When SOM is decomposed and C is largely respired back to the atmosphere as CO_2, the mineralized N becomes available for microbes and plants and this, in turn, could enhance ecosystem productivity (Melillo et al., 2002; Rustad et al., 2001). However, N could also be lost via leaching or directly immobilized by microbes. Not much is currently known about the net effect of soil warming on total N stocks in the soil. This deserves further study so that potential interactions between C and N cycles can be identified and a more comprehensive understanding about whole-ecosystem responses to warming can be developed.

Geothermal areas can help to fill these knowledge gaps because in these areas the whole soil profile has been warmed for long periods of time. When soils are unaffected chemically by geothermal waters, the resultant soil warming may be considered a cost-effective long-term manipulation (O'Gorman et al., 2014). O'Gorman et al. (2014) highlighted the importance of temperature gradients for an in-depth understanding of warming responses including identification of potential tipping points. Another opportunity of geothermal warming is that temperature gradients across the landscape can be identified with different degrees or intensities of warming developed as part of an experimental set-up. In this study, it was possible to take advantage of geothermal soil warming at the Takhini hot springs, located in a subarctic deciduous forest near Whitehorse, Yukon in Canada. It is not known how long the soils have been warmed by the spring, but the spring has been commercially used as a recreational area since around 1907 and we can therefore assume that at least 100 years of warming has occurred. One of the few examples of a comparable site is the ForHot experimental site in Hveragerdir, Iceland (Sigurdsson et al., 2016), where soil has been warmed since an earthquake in 2008 in one valley and for more than 50 years in a neighbouring valley (Walker et al., 2020).

SOM is highly complex and this complexity should be accounted for when trying to predict its dynamics (Lavallee et al., 2019). This is often done by separating multiple components of contrasting behaviour by various fractionation approaches (Lützow et al., 2007). In recent years, physical fractionation methods, and in particular, the separation of size and/or density fractions, have been widely used (Lavallee et al., 2019; Poeplau et al., 2018). This is in line with the current understanding of the major pathways of SOM stabilization (Dynarski et al., 2020), with reduced accessibility of SOM by mineral association as a key mechanism (Dungait et al., 2012; Kögel-Knabner et al., 2008). However, few warming studies have evaluated the response of different SOM fractions to in situ warming (Lavallee et al., 2019). This hampers the in-depth understanding needed for accurate prediction of SOM cycling and transformation in response to global changes that are occurring (Conant et al., 2011). The temperature sensitivity of different SOM fractions has long been a matter of debate, owing to a wide range of different experimental approaches and definitions of temperature sensitivity (Conant et al., 2011; Conen et al., 2006; Karhu et al., 2010; Knorr et al., 2005). Apart from evaluating changes in SOM quality, fractionation can also be used to indicate soil structural changes or reveal prevailing destabilization mechanisms. For example, in the Icelandic geothermal warming experiment mentioned earlier, Poeplau et al. (2016, 2020) detected the depletion of stable aggregates associated with the loss of SOM and concluded that either loss of SOM decreased aggregate stability or weakening of aggregate binding mechanisms led to the destabilization of SOM.

Our aim in this study was to use a natural thermosequence in a subarctic deciduous forest to quantify the effect of long-term whole-profile soil warming on SOC and total soil N stocks and fractions, as well as potential litter decomposition. The latter was used as a proxy to test the hypothesis that SOM losses in the topsoil and subsoil are driven mainly by the warming-induced acceleration of microbial activity.

2 | MATERIALS AND METHODS

2.1 | Study site

The Takhini hot springs (60°52′43.9″N, 135°21′30.7″W, http://takhinihotpools.com/) are located near the Takhini river in south-western Yukon Territory, west of Whitehorse in the discontinuous permafrost region (Smith et al., 2004). The study area is located on the margins of the Whitehorse Trough, a Mesozoic marine basin with sediments and volcanic rocks of Jurassic to Triassic age, locally overlain by glacial and periglacial deposits. At the Takhini hot springs, water is heated by natural decay of plutonic rocks (Langevin et al., 2019) at a depth of several hundred metres and reaches the surface through geological faults (Fraser et al., 2018). This water is captured in a commercial pool with a temperature of 42°C, heating the surrounding soil at a depth of 50 cm from annual temperatures of −4.8°C in winter and 3.7°C in summer (Smith et al., 1998) up to temperatures consistently above freezing. Before the spring's commercial exploitation as a recreational area around 100 years ago, the area was used by the Ta'an Kwäch'än First Nation. There is no scientific work about the exact age of the spring or about the duration of soil warming. We know from old documents such as early photographs and newspapers that the spring was already in use by 1907 and must have delivered hot water to the surface beforehand (http://www.explorenorth.com/library/history/takhini_hotsprings.html). Therefore, we assume that soil warming has occurred for more than hundred years. There is no evidence to suggest that any geothermal water affected the area where the plots were located. At the four plots, the soils had similar soil properties (see Table S1). The geothermal water is rich in calcium and iron, leading to visible precipitates whenever the water comes to the surface. To avoid a chemical influence of the geothermal water on the soils, the plots were established at the back of the spring, where no water directly reaches the surface. The soil pH was similar at all of the plots, which indicated that the soils were not chemically affected by the geothermal water and warming.

The research area is located in the Aspen forest (*Populus tremuloides*, MICHX) on Orthic Eutric Brunisols (Canadian Soil Classification; Mougeot, 1997) that developed from glaciolacustrine deposits and till (Bond et al., 2005), originating from the late Pleistocene Cordilleran Ice Sheet (Duk-Rodkin, 1999). The soil at the experimental site has a loamy to silty-loamy texture (average of 20% sand, 63% silt and 17% clay) and a neutral to alkaline pH_{H20} of between 6.7 and 8.8 (Table S1). Carbonates are present below a depth of approximately 50 cm.

The research site has an annual precipitation of 267 mm and an annual mean temperature of −1.6°C according to Canadian Climate Normals (Environment Climate Change Canada, 2020) using data from 1981 to 2010.

2.2 | Plot selection and soil temperature measurement

Sampling plots were selected by measuring the current soil temperature, which decreased with a distance from the hot spring. The four sampling plots (W1, W2, W3 and W4, with W1 closest and W4 furthest away from the spring), each represented a specific warming intensity, were selected on the basis of relatively undisturbed forest patches on flat terrain. To ensure this, sampling plots had to be small (3 × 3 m^2) due to the infrastructure around the spring. Overall, the resulting thermosequence was of small spatial dimension with very close coordinates: W4 = 60.879159°N/−135.361128°E, W3 = 60.879011°N/−135.360853°E, W2 = 60.879118°N/−135.359916°E and W1 = 60.878867°N/−135.360272°E. The plots were located within 60 m of the spring. At each plot, temperature loggers (Tinytag Plus 2 TGP 4017, Gemini Data Loggers Ltd) were buried at 10 and 50 cm soil depths to log the temperature with a resolution of 2 h for 1 year (July 2019–July 2020). After 1 year of logging, the temperature loggers provided a detailed picture of the soil temperature pattern throughout the year. Figure 1 shows that the plot closest to the hot spring (W1) was continuously warmer than the reference plot (W4), with a maximum temperature difference of 8.6°C at 50 cm depth. As temperature data were obtained for two depths, reference is made to the mean of both depths and the warming intensity compared with the reference plot (W4), which is 7.7°C (W1), 1.8°C (W2) and 0.5°C (W3). At the warmest plot (W1), the temperature dropped below 0°C only in exceptional cases (6 days in January), while all other plots remained frozen for at least part of the winter (Figure 1). While plots W2, W3 and W4 had similar, often overlapping temperature curves at 10 cm depth, the temperature at 50 cm was clearly different among the plots, indicating a greater influence of the geothermal heat source deeper in the soil.

2.3 | Sampling and field measurements

A transect of the four established plots was sampled in July 2019. The litter layer was sampled using a metal cylinder of 12.5 cm diameter (8 cm height) prior to soil coring. The thickness of the litter layer did not exceed 4 cm. A slide hammer-driven soil corer with an auger of 7 cm diameter and 20 cm length was used for soil sampling at four random locations in each plot. The soil cores were divided into five depth increments (0–10, 10–20, 20–40, 40–60 and 60–80 cm). The separate sampling of all depth increments with the 20-cm auger precluded the deformation of soil cores (compaction/stretching) and thus ensured correct volume-based sampling. In two replicates of one plot (W4), the 60–80 cm

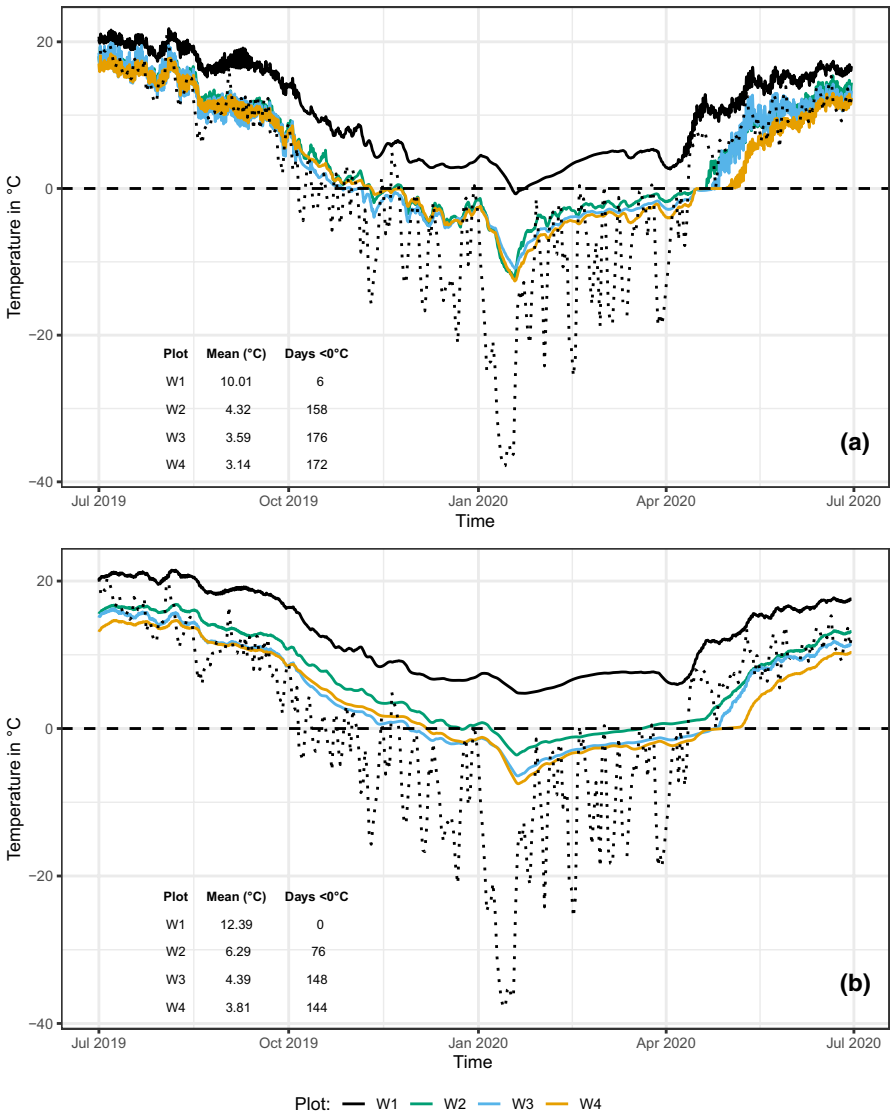

FIGURE 1 Soil temperature over a 1-year period at depths of (a) 10 cm and (b) 50 cm for all four plots (W1–W4), with the dashed line indicating the freezing point and the dotted line indicating air temperature recorded at the closest weather station in Whitehorse (air temperature data provided by the Computer Research Institute of Montréal, 2020)

depth increment could not be sampled due to the high gravel content.

To determine the potential litter decomposition rate, teabags with green tea ('Bio Grüner Tee', Paulsen Tee, Fockbeck, Germany, Charge No. 187896FC) were used (Keuskamp et al., 2013, modified). The teabags were buried at depths of 10 and 50 cm in the centre of each plot (three bags per depth and plot, resulting in 24 teabags) to study warming effects on potential litter decomposition as a proxy for microbial activity. The teabags were tagged and weighed before burying. After 1 year, the teabags were recovered, cleaned, dried at 60°C and weighed again to determine tea mass loss. Six of the 24 teabags could not be recovered.

2.4 | Sample preparation and analyses

The freshly sampled soil was air-dried, weighed, sieved through a 2-mm sieve and weighed again to calculate the fine soil mass and stone content (Equation 1). An aliquot sample of the sieved soil was then shipped to Germany, where all further parameters were measured. The water content of each air-dried sample was determined to correct the fine soil mass estimate by subjecting an aliquot to 105°C oven-drying and calculating the weight difference between air- and oven-dried samples.

For the measurement of pH and texture, the four field replicates of each plot and depth were pooled into one sample per depth increment, resulting in five samples per plot. The pH of each pooled sample was measured in water with a soil:water ratio of 1:5 (10 g soil and 50 g water) after 1-h shaking (ISO 10390, 2005; Table S1). Soil texture was determined for the samples from the second depth increment (10–20 cm) according to DIN ISO, 11277:2002-08, which is based on sieving and sedimentation of suspended fine particles (Köhn, 1929).

Milled aliquots of each sample were used for analysis of SOC, total inorganic carbon and total N analysis by dry combustion with an elemental analyser (LECO TruMac). Samples with a pH_{H2O} > 6.2 were combusted in a muffle furnace prior to dry combustion to determine total inorganic carbon. Milled aliquots of the litter samples were analysed for SOC and N.

2.5 | Fractionation

SOM fractions were isolated in all 78 samples according to the method of Zimmermann et al. (2007) which had been slightly modified by Poeplau et al. (2018). Briefly, 30 g of the bulk soil were dispersed with an ultrasonic probe at 22 J and then wet-sieved with 2.2 L deionized water through a 63-µm sieve (the threshold between silt and sand in the German Soil Classification; Ad-hoc-Arbeitsgruppe Boden, 2005). The fine fraction was then centrifuged and the supernatant fluid was filtered (0.45 µm) and analysed for water-extractable carbon (here referred to as DOC). DOC was measured with a Dimatoc 2000 (Dimatec GmbH, Essen). The remaining silt and clay fraction (S+C) was dried until the weight was constant at 50°C, weighed and analysed for C content. From the S+C fraction, 1 g was used to determine the resistant soil organic carbon (rSOC) and resistant soil nitrogen (rSN) using oxidation with 6% sodiumhypochlorite (NaOCl). In this step, the 1 g sample was stored in a 50-ml centrifuge tube and filled to 45 ml with NaOCl. After shaking, the tubes were left open for 16 h to ensure maximum oxidation and prevent the tubes from bursting due to gas produced by the ongoing oxidation process. Afterwards, the tubes were centrifuged, decanted, washed twice with deionized water and refilled with NaOCl. After three repetitions, the washed sample was dried at 50°C and the remaining material was analysed for C and N content.

The coarse fraction from the wet sieving was dried at 50°C and then weighed. Afterwards, this fraction was mixed with a sodium polytungstate solution adjusted to a density of 1.8 g/cm^3. After mixing and centrifuging, the particulate organic matter (POM) floating on the heavy solution was decanted, washed with deionized water, dried again at 50°C, weighed, milled and analysed for C and N contents. The same procedure was applied for the heavy sand and aggregate fraction (S+A).

This fractionation method leads to a small loss of both sample mass and carbon, and the recovery (sum of all isolated fractions) was measured to be 97% for the initial bulk soil mass and 90% for the initial bulk soil carbon. Due to high carbonate content between 40 and 80 cm, the rSOC fraction could not be accurately evaluated and was not considered at these depths. As the rSOC fraction consisted of less than 1 g, it was not possible to distinguish inorganic C and SOC. The fractionation method developed by Zimmermann et al. (2007) has been applied in other comparable geothermal warming studies (Poeplau et al., 2016, 2020). Furthermore, in a large-scale method comparison with 20 different fractionation methods, this method was found to be among the most successful in isolating pools of distinct turnover rates (Poeplau et al., 2018). The method not only allows for the isolation of POM and mineral-associated OM, which are used in other fractionation methods, but also provides information about soil structure from the S+A fraction, and about desorption and leaching processes by the DOC fraction.

2.6 | SOC stock calculation and mass correction

Considerable variability in the rock fragment fraction was observed across the plots (Table S1). To avoid a bias in SOC stock estimates caused by the high proportion of rock fragments in the soil samples and assuming that this variation was not temperature driven, SOC stocks were calculated as $SOCstock_i$ using the following equations (M2 in Poeplau et al., 2017):

$$BD_{\text{fine soil}} = \frac{\text{mass}_{\text{sample}} - \text{mass}_{\text{rock fragments}}}{\text{volume}_{\text{sample}} - \frac{\text{mass}_{\text{rock fragments}}}{\rho_{\text{rock fragments}}}}, \quad (1)$$

$$SOCstock_i = SOCcon_{\text{fine soil}} * BD_{\text{fine soil}} * depth_i \quad (2)$$

where $\text{mass}_{\text{sample}}$ is the total mass of the sample, $\text{mass}_{\text{rock fragments}}$ is the total mass of the rock fragments (>2 mm), $\text{volume}_{\text{sample}}$ is the volume of the sample, $\rho_{\text{rock fragments}}$ is the density of the rock fragments (assumed to be 2.6 g cm^3), $SOCcon_{\text{fine soil}}$ is the SOC content of the fine soil and $depth_i$ is the sampling depth of the corresponding increment.

As a change in treatments is often accompanied by changes in horizon thickness and bulk density, a mass correction of the measured SOC concentration is needed (Ellert und Bettany, 1995). The correction of SOC stocks for bulk density was performed according to Poeplau et al. (2011), where the soil mass of the lightest core (0–80 cm) is used as the reference soil mass, and soil and C masses in the other cores are adjusted relative to it. In this case, the mean of the four cores from the reference plot (W4) was used. Mass corrections along the whole profile affect each depth increment and lead to a change in the depth of these increments. This makes it difficult to compare SOC stocks of specific depth increments. To avoid overcorrection, we calculated the mass correction in a first step only for the two uppermost depth increments (0–10 and 10–20 cm), which are herein referred to as topsoil, and in a second step for all five depth increments, which are referred to as subsoil. To obtain mass-corrected subsoil SOC stocks, we subtracted the corrected topsoil SOC stocks from the corrected whole-profile SOC stocks. Therefore, our use of terms 'topsoil' and 'subsoil' does not refer to pedogenic or diagnostic horizons, and topsoil is representative of the SOM-rich rooting zone of the investigated soil.

2.7 | Statistical analysis

All statistical analyses were conducted using R version 3.6.1 (R Core Team, 2019) with the packages readxl (Wickham & Bryan, 2019), openxlsx (Schauberger & Walker, 2020), ggplot2 (Wickham, 2016), ggpubr (Kassambra, 2020), dplyr (Wickham et al., 2020), plyr (Wickham, 2011), reshape2 (Wickham, 2007), gridExtra (Auguie, 2017) and vegan (Oksanen et al., 2019). In order to test the sensitivity of SOC and N stocks, contents and SOC fractions to soil warming, linear and logarithmic regression models were applied for each depth and variable, from which the best fit (best R^2) was chosen (Tables S3–S6). Furthermore, Spearman's correlation coefficient was calculated to test for rank correlation between soil temperature and average stocks of C and N.

To test for differences in SOC and N fraction composition between the plots, an analysis of similarity (ANOSIM) was performed

with the vegan-package (Oksanen et al., 2019). The calculated *R* values give the measure of dissimilarity between all four groups, with corresponding *p*-values to account for statistical significance ($p < 0.05$). This means that ANOSIM could be used to analyse a change in the distribution of fractions between plots.

Furthermore, the ratio of the SOC and N contents between the warmed plots and the reference plot was calculated as the response ratio (RR) to quantify the accumulation or depletion in response to warming:

$$RR = \frac{X_{warm}}{X_{ref}} \quad (3)$$

where RR is the response ratio, X_{ref} is the content of SOC or N in the reference plot and X_{warm} is the content of SOC or N in the warmed plot.

The decomposition of the green tea as a function of soil temperature was best described by the following model:

$$Y = n + \log(x) * m \quad (4)$$

where *Y* is the decomposition within 1 year; *x* is the mean annual soil temperature; and *n* and *m* are the fitted parameters of the model function.

The temperature data were processed with a Hampel filter using a moving window of eight measurements and the twofold median absolute deviation (Pearson et al., 2016). The Hampel filter corrects for outliers in the data, such as temperature changes in several degrees between 2 h, while keeping the natural intraday variations in the data. For comparisons with air temperature, the data of daily mean air temperatures from Whitehorse were used (Computer Research Institute of Montréal, 2020).

3 | RESULTS

3.1 | Bulk soil C and N

In all plots, SOC and N contents were highly variable (Figure 2a,b). As expected, SOC contents were highest in the reference plot and lowest in the warmest plot (Figure 2a). In all plots, SOC decreased exponentially with depth. Consistent with SOC contents, the whole-profile SOC stocks were also highest in the reference plot (Figure 3a). The warmest plot, W1 (+7.7°C), contained on average 14.32 Mg ha^{-1} (27%) less SOC in the whole profile (0–80 cm) than the reference plot. Assuming a linear loss of SOC over the temperature range between the warmest plot and the reference plot, this is equivalent to a loss in SOC of 1.86 Mg ha^{-1} or 3% per °C warming. In the 0–20 cm topsoil layer, the difference in SOC stock between the warmest plot and the reference was 4.79 Mg ha^{-1} (which represents a loss of 16%), while the subsoil lost 9.53 Mg ha^{-1} (34%; see

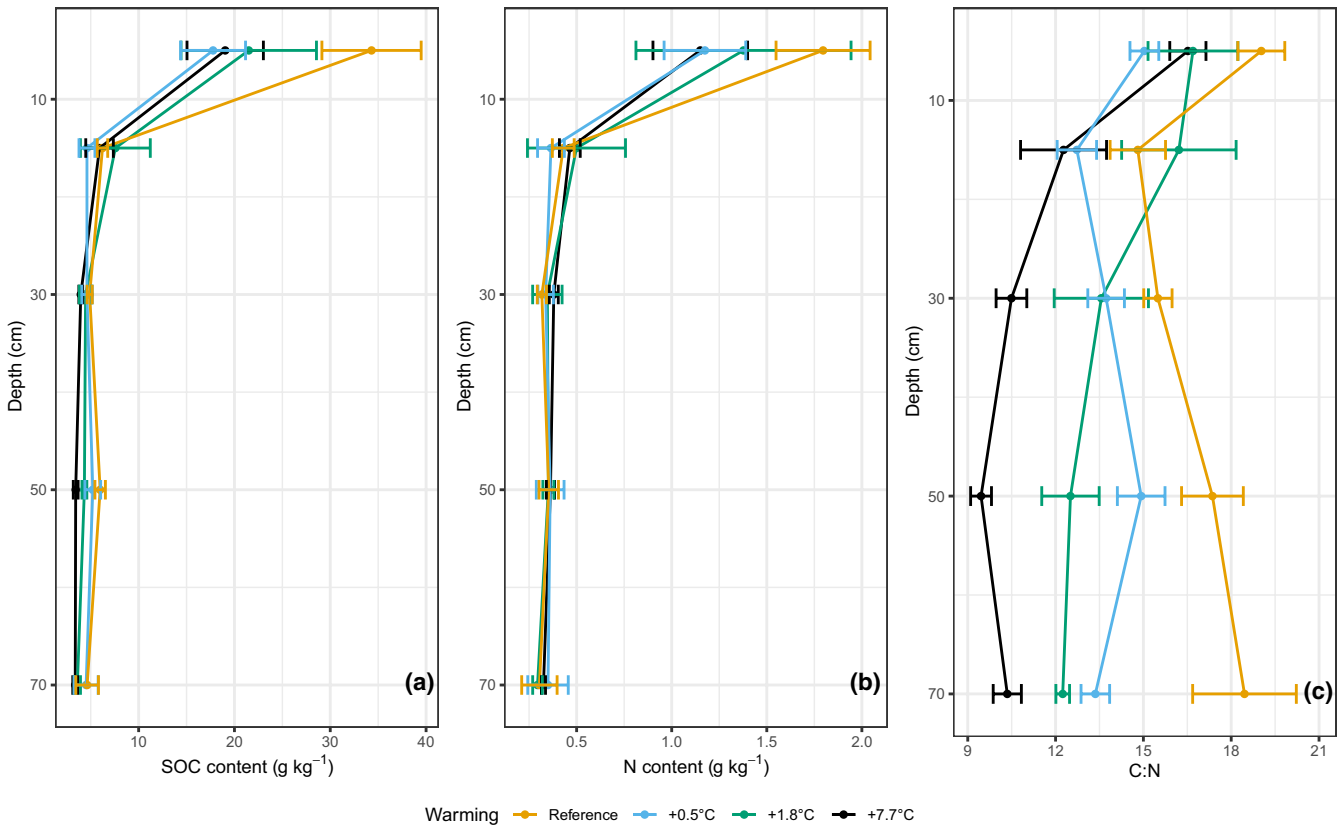

FIGURE 2 Depth profiles with mean (points) and standard error (horizontal bars) of (a) soil organic carbon (SOC) content, (b) nitrogen (N) and (c) C:N ratio

Table S2 and Figure 3a). The C:N ratio (Figure 2c) was strongly related to temperature and decreased with increasing temperature; this effect was strongest in the subsoil. N stocks (Figure 3b) remained constant with warming, indicating that no N was lost from the soil due to warming. Litter C and N stocks remained unaffected by warming (Table S2; Figure 3a,b). Moreover, no statistically significant effects of warming were detected on bulk soil C and N contents and stocks, due to high within-plot variability. However, significant ($p < 0.05$) correlations, using the Spearman's rank test, were found between temperature and average subsoil SOC stocks (Rho = −0.62, $p = 0.01$) and whole-profile SOC stocks (Rho = −0.52, $p = 0.04$), where no significant correlation was observed for the topsoil SOC (Rho = −0.23, $p = 0.39$). Soil N was not significantly correlated with temperature.

A response ratio (RR) < 1 indicates a loss in SOC or N content in the warmed plot relative to the reference plot, whereas a RR > 1 indicates that SOC or N had accumulated in the warmed plot. Since RR is based on contents (g kg^{-1}), it is independent from any correction of soil mass. Across plots, the RR (Table 1) values decreased with warming but did not change with depth indicating that changes in SOC contents were related to warming but not to depth in the soil profile. In contrast to the SOC, the RRs of soil N contents did not decrease with warming, but it appears that there was a slight relocation of N to deeper soil layers because the RR values indicated a loss in the uppermost layer with a concomitant gain in deeper layers.

3.2 | SOM fractions

The sum of C in all fractions tended to decrease with increasing soil temperature in three out of four depth increments (Figure 4a), but regression analysis indicated that no significant trends were found. A significant effect of warming was found for the stocks of POM at 20–40 and 40–60 cm layers (negative) and for rSOC at 40–60 cm, as well as for the C concentrations at 20–40 cm (POM and rSOC) and 40–60 cm (POM, S+C, DOC). A detailed description of these results is provided in Tables S3 and S4. Carbon stored in POM decreased with warming across all depths, except for 10–20 cm, where it remained constant (Figure 4a). The other fractions showed minor responses, except for the S+C fraction. Carbon stored in the S+C fraction showed an inconsistent response to warming, with an increase at 60–80 cm, a decrease at 40–60 cm but was unchanged at other depths. The relative contribution of C in the different fractions (Figure 4b) revealed a more consistent pattern. With warming, POM showed again the strongest response of all fractions. In contrast, the proportion of the S+C fraction tended to increase with warming in all plots. No clear difference between the response of the oxidation-resistant rSOC fraction and the oxidizable S+C fraction was observed.

Across all fractions and depth increments, the response to warming was greatest in the POM fraction. Over the entire 80 cm soil profile, POM-C accounted for about half of the bulk SOC stock in the reference plot, and its share became significantly smaller with every warming step (Figure 3c). In contrast, the stocks of the other fractions remained almost constant throughout all warming steps. As depicted in Figure 3c, the loss of POM was driving total SOC loss. Over the whole soil profile, POM was depleted by 13.94 Mg ha^{-1}, while the other fractions contributed much less, with less than 1 Mg ha^{-1} for each fraction. After POM, the DOC fraction had the greatest proportional loss with 0.24 Mg ha^{-1}, which equals 15% of the DOC in the reference plot.

Nitrogen stocks were not reduced by warming, as shown in Figure 3b and the constant RR values across plots (Table 1). The results of the ANOSIM (Table 2) and the distribution of N between the fractions (Figure 5) show a significant shift of 0.55 Mg ha^{-1} N

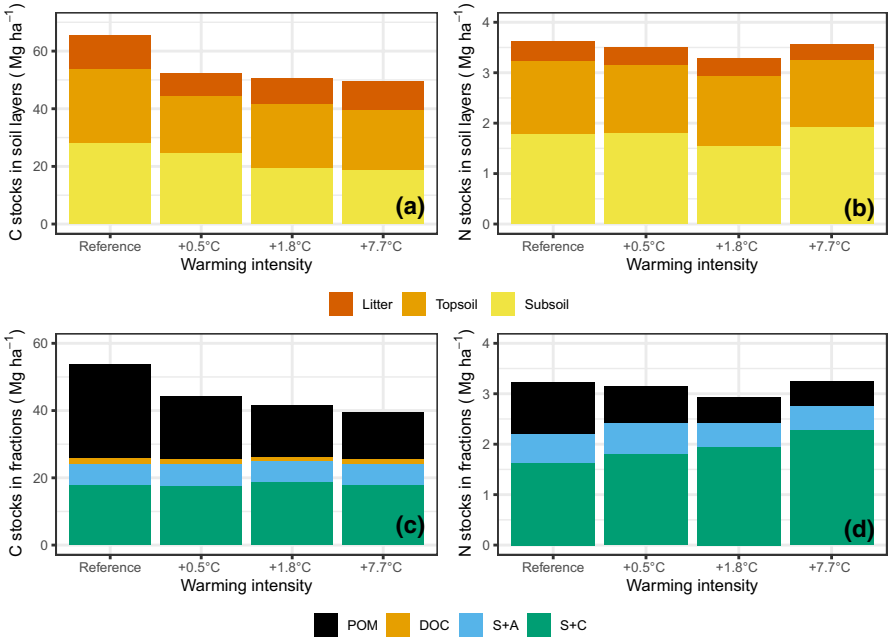

FIGURE 3 (a) Contribution of litter layer, topsoil (0–20 cm) and subsoil (20–80 cm) C to total C stocks. (b) Contribution of litter layer, topsoil and subsoil N to total N stocks. All displayed stocks are corrected to the reference soil mass of topsoil and subsoil. (c) Contribution of the C fractions (DOC, dissolved organic matter; POM, particulate organic matter; S+A, sand and stable aggregates; S+C, silt and clay) to the total C stocks. (d) Contribution of the N fractions (POM, S+A and S+C) to total N stocks

from POM to the S+C fraction and an overall accumulation of N in the S+C fraction of 0.64 Mg ha^{-1}, representing a 40% increase in N in the S+C fraction (Figure 3d). As a result of changes in SOC and no concomitant changes in N, the C:N ratio became narrower with warming (Figure 2c); this change was consistent across depth increments but was most pronounced in the subsoil. Finally, for N stocks (Figures 3b and 5a), a slight distribution shift from topsoil to subsoil with warming was observed. In the reference plot, 45% of soil N (1.46 ± 0.17 Mg ha^{-1}) was stored in the topsoil and 55% (1.77 ± 0.16 Mg ha^{-1}) in the subsoil. Whereas in the warmest plot, 41% of N (1.34 ± 0.23 Mg ha^{-1}) was stored in the topsoil and 59% (1.91 ± 0.08 Mg ha^{-1}) in the subsoil.

The ANOSIM (Table 2) revealed that there was a significant change in the distribution of SOC and total N among the five fractions, suggesting there were distinct responses to warming. At least for N, which did not change in absolute amounts, this indicates that it was transferred between fractions.

TABLE 1 Response ratio (RR) of C and N contents between the reference and the three warmed plots for each depth increment

	C			N		
	+0.5°C	**+1.8°C**	**+7.7°C**	**+0.5°C**	**+1.8°C**	**+7.7°C**
0–10 cm	0.52	0.63	0.55	0.65	0.77	0.64
10–20 cm	0.74	1.22	0.95	0.85	1.16	1.08
20–40 cm	0.94	0.91	0.81	1.06	1.09	1.20
40–60 cm	0.87	0.73	0.57	1.02	0.99	1.03
60–80 cm	0.98	0.78	0.73	1.15	0.97	1.07

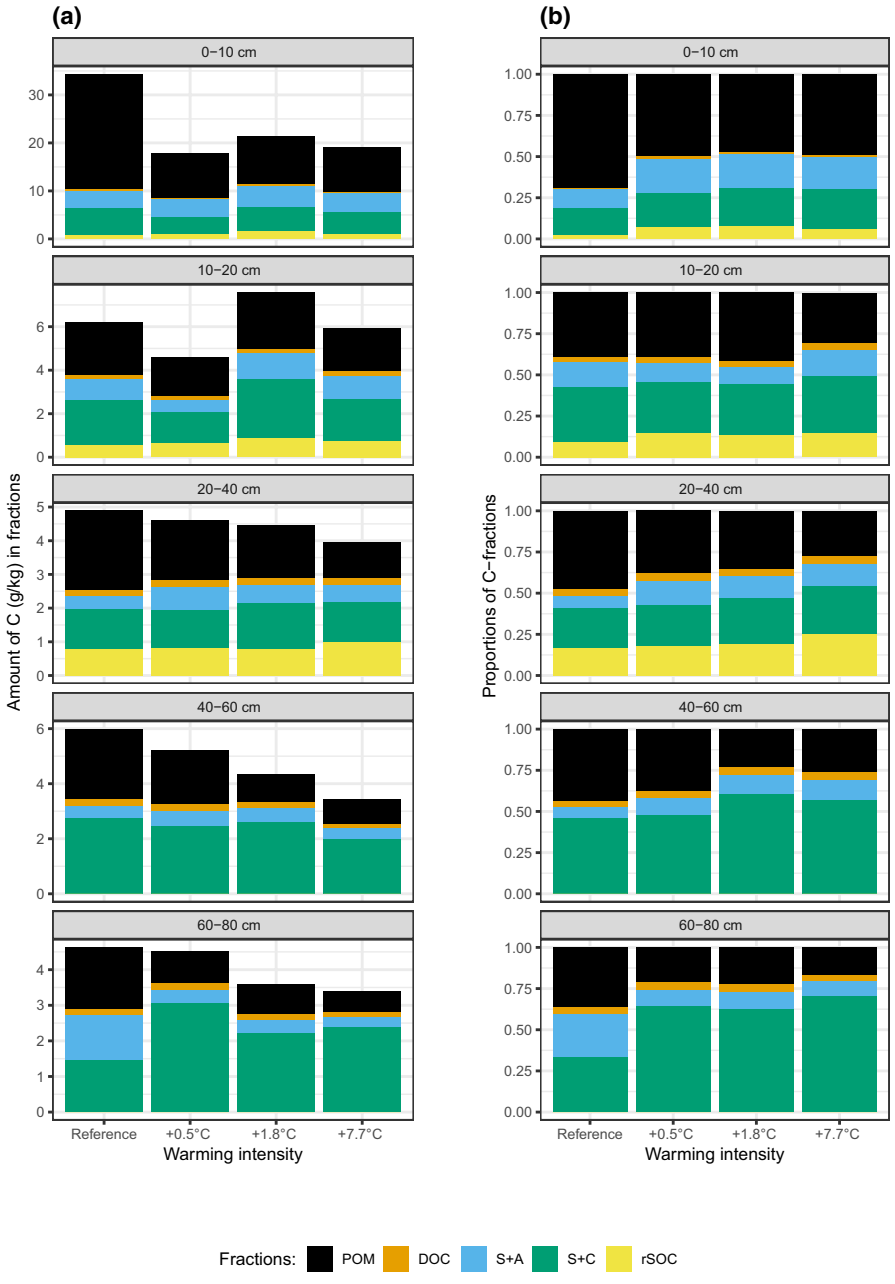

FIGURE 4 Bar plots of amount of C (a) and proportional share of C (b) in particulate organic matter (POM), dissolved organic carbon (DOC), sand and stable aggregates (S+A), silt and clay (S+C) and resistant organic carbon (rSOC) in relation to soil warming

TABLE 2 Results of the ANOSIM for the relative composition of the soil organic matter (SOM) fractions in C and N for each depth increment

	Relative distribution of C		Relative distribution of N	
Depth	***R***	***p***	***R***	***p***
0–10 cm	0.75*	0.035	0.75*	0.03
10–20 cm	−0.052	0.643	0.083	0.291
20–40 cm	0.635*	0.023	1*	0.001
40–60 cm	0.594	0.05	0.542*	0.037
60–80 cm	1*	0.033	1*	0.027

*Significant differences between the warming plots with $p < 0.05$.

3.3 | Litter decomposition

The teabag experiment indicated that temperature had a significant effect on litter decomposition rates (Figure 6). Overall, the tea litter at 50 cm depth was less decomposed and observations were more variable than at 10 cm. The intercept of the regression equation shows that decomposition is generally lower at 50 cm than at 10 cm (54.5 at 50 cm and 38.1 at 10 cm), whereas the slope coefficients indicate a similar response to warming at both depths (12.65 at 50 cm and 12.38 at 10 cm). The difference in R^2 between 50 and 10 cm indicates that observations at 50 cm depth had a higher uncertainty than observations at 10 cm depth. The *p*-values of the regressions were 0.002 at 50 cm and <0.001 at 10 cm.

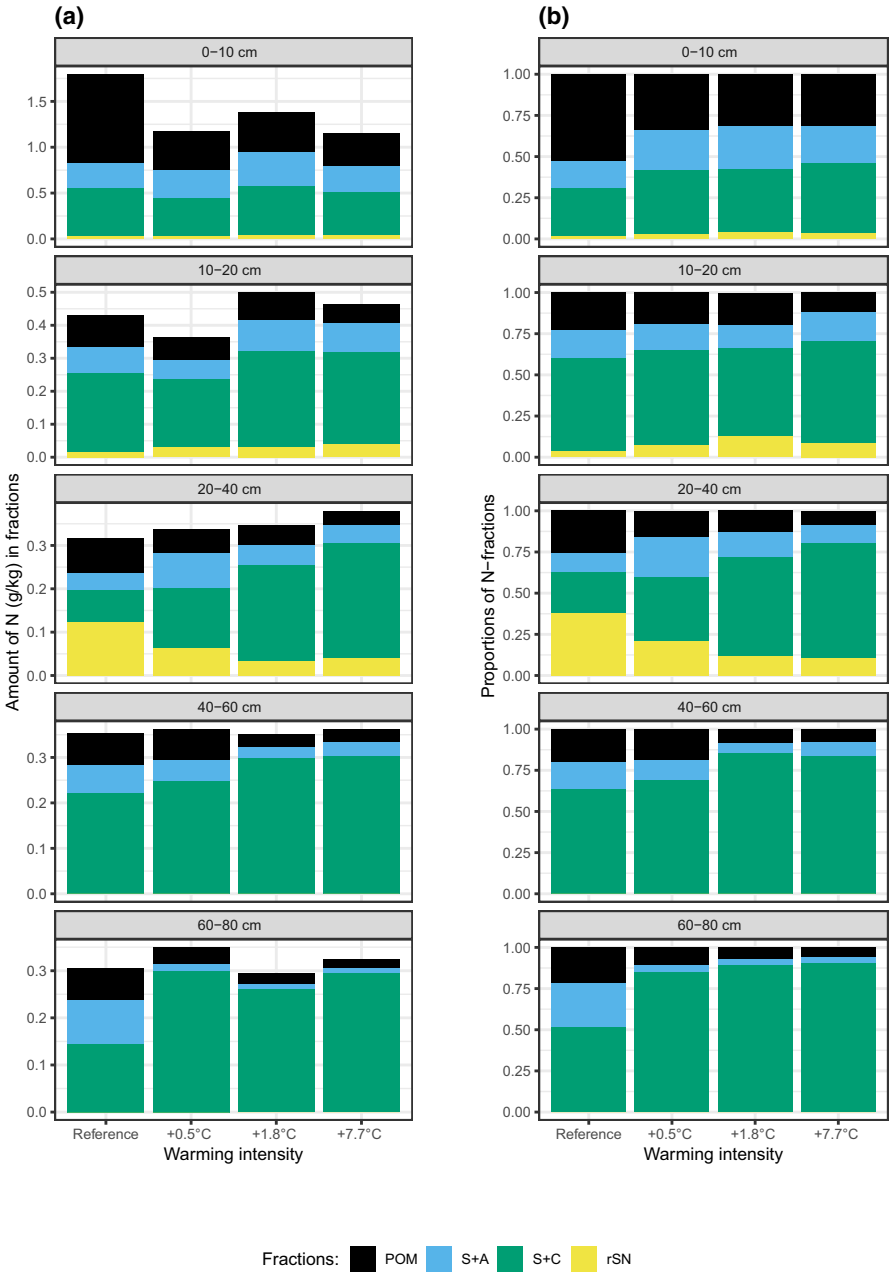

FIGURE 5 Bar plots of amount of N (a) and proportional share of N (b) in particulate organic matter (POM), sand and stable aggregates (S+A), silt and clay (S+C) and the resistant organic carbon fraction (rSN) in relation to soil warming

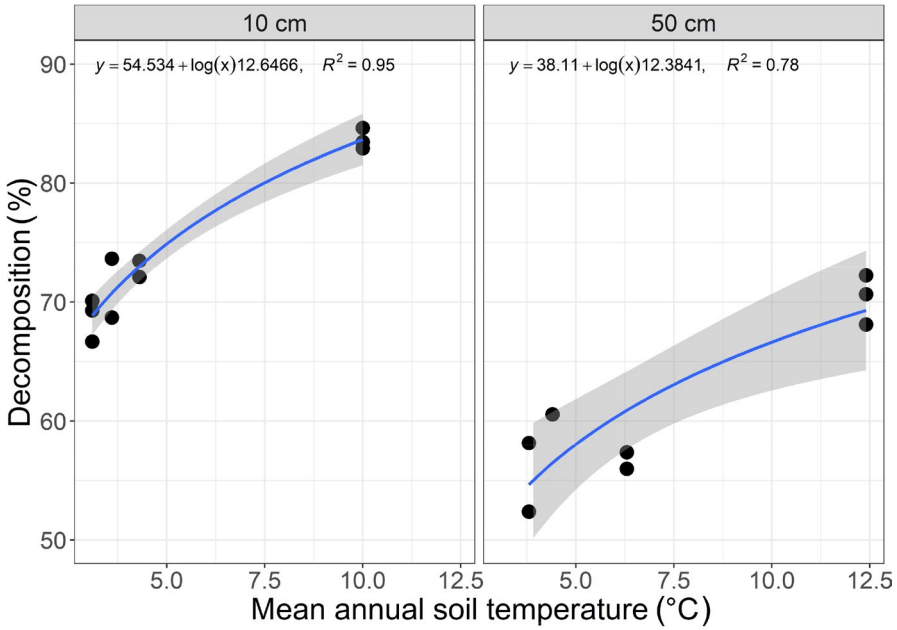

FIGURE 6 Decomposition of litter (green tea) at 10 and 50 cm depths after being buried for 1 year

4 | DISCUSSION

4.1 | Response of bulk SOM

Bulk SOC stocks showed a long-term loss of approximately 1.86 Mg ha^{-1} $°C^{-1}$, or 27%, with a maximum warming intensity of 7.7°C. This total loss was considerably lower than the predictions of Crowther et al. (2016), who reported losses of up to 30 Mg ha^{-1} under conservative climate change scenarios by 2050. These losses were the result of linear extrapolation of data from mostly short-term warming experiments. But this approach may overestimate what actually occurs over the long term (van Gestel et al., 2018; Walker et al., 2020). Studies with a relatively long time span of observation (e.g. Poeplau et al., 2020, Melillo et al., 2002, 2017) reported results that are consistent with our findings. Melillo et al. (2017) observed a long-term pattern of rapid SOC loss at the start of soil warming but reaching a new equilibrium between SOC mineralization and build-up later in the experiment. They reported that the largest loss of bulk SOC occurred within the first 10 years after the onset of heating. It has been suggested that continued heating might lead to a decrease in microbial biomass and changes in microbial growth and turnover without losing more SOC (Walker et al., 2018). Thus, the assumption that short-term warming responses can be extrapolated to longer time periods (Crowther et al., 2016) might not be valid (Walker et al., 2020). Our results are consistent with the observations of Melillo et al. (2017), because even after more than 100 years of warming, the SOC losses we observed were not greater than those observed in other studies. Furthermore, Poeplau et al. (2020) observed SOC losses between 3.6% and 4.5%$°C^{-1}$ in topsoil and subsoil after 10 years of warming, which is slightly higher than our observed whole-profile loss of 3%$°C^{-1}$ after at least 100 years of warming. If these two subarctic forest ecosystems are comparable, then the results from the two studies would provide evidence that a new equilibrium is rapidly reached after several years of warming. But direct evidence for such response to warming is still limited. Knowledge of the temporal dynamics of SOC immediately after the onset of warming is necessary to correctly interpret the findings of in situ warming experiments.

The results of our study suggest that SOC throughout the soil profile was reduced by warming. Even if the loss in the subsoil was overestimated by calculations to correct for comparable soil masses, the results of this study indicate that subsoil SOC was strongly reduced by warming. This is because firstly, the C fractions showed a strong change in their relative shares in the deepest soil horizon, which cannot be explained by correction for soil mass. Secondly, the RR values of SOC contents, which are independent of soil mass correction, indicate there was a warming-induced response in both topsoil and subsoil C. The SOC losses we observed in the subsoil highlight why whole-profile studies are important for determining the overall climate C cycle feedback (Crowther et al., 2016; Hicks Pries et al., 2017; Liebmann et al., 2020).

The narrowing C:N ratio revealed that a change in chemical composition of SOM occurred with warming. This can be interpreted as a shift from more fresh plant-derived OM with a wide C:N ratio (Ferlian et al., 2017), to a stronger microbial influence on OM, which usually results in a narrower C:N ratio (Hassink, 1994). Such a shift in SOM quality towards more microbial-derived compounds after whole-profile soil warming was recently also observed by Ofiti et al. (2021), who used molecular biomarkers to characterize the changes in SOM quality after warming. This interpretation is supported by the relative gains of the mineral fractions, since much of the C stabilized in those fractions probably consist of microbial residues (Hassink, 1994; Ludwig et al., 2015). The increasing differences of the C:N ratio with depth and warming across plots could indicate that less fresh plant-derived organic matter reaches the subsoil in the warmer plots, which would also be in line with the findings of

Ofiti et al. (2021). This may be due to: (i) greater evaporation at the surface of warmer soils and thus less leaching of fresh DOC from the topsoil; (ii) lower root growth into deeper soil layers, due to greater availability of N in the topsoil in warmer plots; or (iii) changes in turnover of fresh OM. To understand these processes in detail, a closer look at soil water content, root abundance and net primary production would be necessary. It is noteworthy that the soil N stock was not affected by warming; this indicates that increased decomposition of organic matter did not lead to N loss from the soil. This in turn suggests more efficient cycling of N in warmer soils. Our hypothesis regarding SOM losses in both topsoil and subsoil due to warming-induced acceleration of decomposition was confirmed, but only for C, because bulk N stocks were unaltered with warming.

The lack of any loss in N stocks as result of soil warming in this study contradict the findings of Li et al. (2018), who observed considerable losses of N after soil warming by 5°C. But their study was conducted in a subtropical ecosystem with a monsoon climate, so the question arises as to whether more N leaching would occur in warmer and wetter conditions than in the continental subarctic ecosystem studied here. Our findings are consistent with those of Melillo et al. (2002), who observed increased N mineralization after warming by 5°C for 10 years, but with no leaching or gaseous loss of N. Less leaching of N and more N in the soil profile could have fostered greater net primary productivity, which might have compensated for C losses, for example, by increased root-derived C input. Indeed, in the warmest plot (W1), more herbaceous ground vegetation was observed than in the reference plot, which is indicative of a change in ecosystem productivity. This would however stand in contrast to the observation of increased silt and clay-associated N and reduced POM-N, which makes it more likely that microbes were more competitive for the increased available N than plants.

4.2 | Response of different soil organic matter fractions

We found a response to long-term warming by the different SOM fractions to be in the following order: POM > bulk soil > DOC > S+A > SC-rSOC > rSOC. We ascribe the differences among the fractions to differences in accessibility (location in the soil matrix) and chemical composition of the various SOM fractions. This is in agreement with previous studies in a naturally warmed subarctic spruce forest (Poeplau et al., 2020) and matches the observed responses to land use change (Poeplau & Don, 2013). The fact that detected SOC losses can be almost entirely assigned to losses in the POM fraction confirms that this unprotected pool of SOM is highly vulnerable to environmental change (Del Galdo et al., 2003; Lajtha et al., 2014). The amount of mineral-associated SOC (i.e. that in the S+A, S+C and rSOC fractions) was the same in all soils along the warming gradient. This is in contrast to the findings reported in a similar geothermal warming experiment in Iceland, where SOC in the S+A fraction, as well as aggregates, declined strongly with warming; in this study, the silt and clay-associated SOC was lost at a similar rate as bulk SOC (Poeplau et al., 2016, 2020). However, this does not imply that those fractions were not affected by warming in the present study. It is noteworthy that we observed a strong accumulation of N in the S+C fraction because while POM lost 0.55 Mg N ha^{-1} (−52%) and S+A lost 0.07 Mg N ha^{-1} (−12.5%), S+C was enriched by 0.8 Mg ha^{-1} (+60%) in soils along the warming gradient. The microbial turnover pathway is suggested to be a main pathway of SOC stabilization and formation of mineral-associated organic matter (Cotrufo et al., 2019; Sokol et al., 2019). It is also likely that, in addition to increased turnover of POM and N availability, microbial growth and turnover were enhanced (Walker et al., 2018). This may have finally led to an increased flux of microbial-derived organic matter to the S+C fraction, potentially compensating for losses or reduced inputs of plant-derived organic matter. In a recent review, Angst et al. (2021) found a positive correlation between the amino sugar content in mineral-associated organic matter and mean annual temperature, which might support this accumulation. An alternative mechanism for the accumulation of N in S+C could be the adsorption of ammonium, particularly to clay minerals following increased N mineralization (Nieder et al., 2011). Few studies have focussed on the impact of warming on N processes in soil. Ineson et al. (1998) found no significant effect of heating on N leaching in a mountainous ecosystem under a tundra climate. They concluded that any warming-induced increase in decomposition is compensated by an increased plant uptake of N. Rustad et al. (2001) summarized the results of studies on N mineralization after soil warming and found that warmer temperatures increased N mineralization, with subsequent microbial uptake and immobilization of the mineralized N. They concluded that these processes would eventually increase plant productivity and cause a shift of N between different pools, which is consistent with our results.

4.3 | Potential litter decomposition

The teabag experiment allowed us to directly quantify temperature effects on potential litter decomposition and thus microbial activity. Mass loss of the teabags was accurately described by a logarithmic model. The temperature-dependent pattern of litter decomposition was very similar at 10 and 50 cm depths, as shown by the regression model, while the teabags at 50 cm showed lower mass losses than teabags at 10 cm. Other whole-profile studies (Hicks Pries et al., 2017; Nottingham et al., 2020) also observed that subsoils have a similar temperature sensitivity than topsoils, supporting our findings.

The lower mass loss at 50 cm depth indicates that microbial communities in the subsoil responded similar to warming as those in the topsoil, but were less abundant and/or less active, possibly because of lower substrate availability. The results of this short-term (1 year) incubation experiment with green tea as a relatively labile substrate revealed a similar response to that of the total, whole-profile SOC stock after centuries of warming. The mass loss of green tea in the warmest plot was 15% higher than that in the reference plot, and total SOC was reduced by approximately 25% in the most extreme warming intensity as compared with the reference. The similarity of

these values indicates that long-term SOC losses were most likely driven by increased microbial activity and that potential shifts in organic matter inputs did not compensate much of these respiratory losses. However, this might also be related to the experimental limitation of this study, namely that only the soil, not the whole ecosystem, was warmed, which could have additional effects on the aboveground part of the ecosystem. We conclude that the temperature effect on mass loss of tea adds support to our hypothesis that SOM losses are driven by warming-induced acceleration of microbial activity.

4.4 | Implications for SOC dynamics under climate change and further research

With regard to understanding climate change effects on ecosystem C fluxes, an experimental shortcoming of this and similar studies is that only the soil, and not the aboveground part of the ecosystem, was warmed. The response of net primary productivity to warming and CO_2 fertilization, especially in combination with potentially increased N availability, might compensate for the C losses from the soil (Song et al., 2019) to some extent. This was not the case in our study, since relative SOC losses appear to be consistent with potential litter decomposition rates as shown by mass losses in tea litter. Furthermore, this study also highlights the experimental difficulties in detecting warming effects. While the warming effects on SOM stocks and fractions were consistent across the warming gradient, hardly any statistically significant differences were detected, even at a warming intensity of 7.7°C, due to high intra-plot variability. This implies that large sample sizes and strong warming treatments are necessary in order to detect significant changes (Poeplau et al., 2016; Schöning et al., 2006). Nevertheless, the use of natural soil warming gradients presents a unique opportunity to study processes in an undisturbed natural setting. The Pacific Climate Impacts Consortium (PCIC) projects a rise in annual mean temperature of between 1.8 and 2.1°C (depending on the emission scenario) for the period 2021–2050 and of 2.9–4.2°C for the period 2051–2080, with the strongest warming during winter, resulting in a shorter frost period and less snow cover. Precipitation is expected to rise by 8%–9% between 2021 and 2050, and by 18%–20% between 2051 and 2080 (PCIC, 2014). Using the observed C loss of 1.86 Mg ha^{-1} $°C^{-1}$, the projected rise in mean annual temperature in the study area could lead to a SOC loss of 3.3–3.9 Mg ha^{-1} or 5.4–7.8 Mg ha^{-1}, respectively, depending on the emission scenario. The loss of SOC in the form of CO_2 contributes not only to climate change, but also decreases overall soil quality and productivity (Larsbo et al., 2016). A possible structural change of the soil such as a greater decay of stable aggregates (Poeplau et al., 2020) might affect soil water flow and solute transport, which play an important role in soil respiration and plant growth, especially in semi-arid areas such as the Yukon Territory. The questions of structural changes in the soil should be studied in more detail in undisturbed soil columns. The recycling of N may change the SOM chemical composition, which in turn could affect microbial community composition and metabolism (Manzoni, 2017; Takriti et al., 2018). Recently, Ofiti et al. (2021) also found that SOM in warmed soil was altered in its chemical composition and comprised more microbial-derived compounds. They related this to reduced plant-derived inputs and increased microbial decomposition of organic matter. We assume that this is similar at our study site. However, insights on warming-induced changes in plant inputs and organic matter quality will be necessary to fully understand the opposing trends in C and N stocks we observed. Nevertheless, the use of natural soil warming gradients presents a unique opportunity to study processes in an undisturbed natural setting and are therefore valuable for improving our understanding of ecosystem responses to warming.

ACKNOWLEDGEMENTS

We thank Garry Umbrich, the owner of the Takhini Hotpools for sampling permission, introducing us to the site and his many helpful insights. We are very grateful to Whitehorse locals Jeannie McLorie and Dawson Smith for collecting the teabags and temperature loggers from the plots in their free time, after the pandemic made travelling impossible in summer 2020. We also thank Claudia Wiese and the Thünen Laboratory for Soil Monitoring for processing their samples. Finally, we are also grateful to the Ta'an Kwäch'än First Nation for permitting this scientific work on their traditional territory. This study is part of the 'Breaking the Ice' project funded by the German Research Foundation, grant number 401106790. Funding for E.G. was provided by the Science & Technology Branch of Agriculture & Agri-Food Canada [Project J-001756 'Biological Soil Carbon Stabilization'].

DATA AVAILABILITY STATEMENT

All data used for this study, including an R script to reproduce the presented results, can be found at https://doi.org/10.5281/zenodo.4954979.

ORCID

Tino Peplau https://orcid.org/0000-0001-7181-7331
Julia Schroeder https://orcid.org/0000-0003-3625-104X
Edward Gregorich https://orcid.org/0000-0003-3652-2946
Christopher Poeplau https://orcid.org/0000-0003-3108-8810

REFERENCES

Aaltonen, H., Palviainen, M., Zhou, X., Köster, E., Berninger, F., Pumpanen, J., & Köster, K. (2019). Temperature sensitivity of soil organic matter decomposition after forest fire in Canadian permafrost region. *Journal of Environmental Management*, *241*, 637–644. https://doi.org/10.1016/j.jenvman.2019.02.130

Ad-hoc-Arbeitsgruppe Boden. (2005). Bodenkundliche Kartieranleitung. Mit 103 Tabellen und 31 Listen. Unter Mitarbeit von Herbert Sponagel. 5., verbesserte und erweiterte Auflage. Stuttgart: E. Schweizerbart'sche Verlagsbuchhandlung (Nägele und Obermiller).

Angst, G., Mueller, K. E., Nierop, K. G. J., & Simpson, M. J. (2021). Plant- or microbial-derived? A review on the molecular composition of stabilized soil organic matter. *Soil Biology and Biochemistry*, *156*, 108–189. https://doi.org/10.1016/j.soilbio.2021.108189

Auguie, B. (2017): gridExtra: Miscellaneous functions fpr "grid" graphics. Version R package version 2.3. https://CRAN.R-project.org/package=gridExtra

Bond, J. D., Morison, S., & McKenna, K. (2005). *Surficial geology of upper laberge (1:50 000 scale)*. Yukon Geological Survey. Geoscience Map 2005-8.

Carey, J. C., Tang, J., Templer, P. H., Kroeger, K. D., Crowther, T. W., Burton, A. J., Dukes, J. S., Emmett, B., Frey, S. D., Heskel, M. A., Jiang, L., Machmuller, M. B., Mohan, J., Panetta, A. M., Reich, P. B., Reinsch, S., Wang, X., Allison, S. D., Bamminger, C., … Tietema, A. (2016). Temperature response of soil respiration largely unaltered with experimental warming. *Proceedings of the National Academy of Sciences of the United States of America*, *113*(48), 13797–13802. https://doi.org/10.1073/pnas.1605365113

Computer Research Institute of Montréal. (2020). *Climate data from Whitehorse auto station*. Computer Research Institute of Montréal (Ed.). Author. https://climatedata.ca/download/

Conant, R. T., Ryan, M. G., Ågren, G. I., Birge, H. E., Davidson, E. A., Eliasson, P. E., Evans, S. E., Frey, S. D., Giardina, C. P., Hopkins, F. M., Hyvönen, R., Kirschbaum, M. U. F., Lavallee, J. M., Leifeld, J., Parton, W. J., Megan Steinweg, J., Wallenstein, M. D., Martin Wetterstedt, J. Å., & Bradford, M. A. (2011). Temperature and soil organic matter decomposition rates – Synthesis of current knowledge and a way forward. *Global Change Biology*, *17*(11), 3392–3404. https://doi.org/10.1111/j.1365-2486.2011.02496.x

Conen, F., Leifeld, J., Seth, B., & Alewell, C. (2006). Warming mineralises young and old soil carbon equally. *Biogeosciences*, *3*(4), 515–519. https://doi.org/10.5194/bg-3-515-2006

Cotrufo, M. F., Ranalli, M. G., Haddix, M. L., Six, J., & Lugato, E. (2019). Soil carbon storage informed by particulate and mineral-associated organic matter. *Nature Geoscience*, *12*(12), 989–994. https://doi.org/10.1038/s41561-019-0484-6

Crowther, T. W., Todd-Brown, K. E. O., Rowe, C. W., Wieder, W. R., Carey, J. C., Machmuller, M. B., Snoek, B. L., Fang, S., Zhou, G., Allison, S. D., Blair, J. M., Bridgham, S. D., Burton, A. J., Carrillo, Y., Reich, P. B., Clark, J. S., Classen, A. T., Dijkstra, F. A., Elberling, B., … Bradford, M. A. (2016). Quantifying global soil carbon losses in response to warming. *Nature*, *540*(7631), 104–108. https://doi.org/10.1038/nature20150

Del Galdo, I., Six, J., Peressotti, A., & Cotrufo, M. F. (2003). Assessing the impact of land-use change on soil C sequestration in agricultural soils by means of organic matter fractionation and stable C isotopes. *Global Change Biology*, *9*(8), 1204–1213. https://doi.org/10.1046/j.1365-2486.2003.00657.x

DIN ISO 11277:2002-08, 2002: DIN ISO 11277:2002-08. (2002–08). Bodenbeschaffenheit_- Bestimmung der Partikelgrößenverteilung in Mineralböden - Verfahren mittels Siebung und Sedimentation (ISO_11277:1998_+ ISO_11277:1998 Corrigendum_1:2002).

Duk-Rodkin, A. (1999). Glacial limits map of Yukon Territory. Open File 3694, Indian and Northern Affairs Canada Geoscience Map 1999-2: Geological Survey of Canada.

Dungait, J. A. J., Hopkins, D. W., Gregory, A. S., & Whitmore, A. P. (2012). Soil organic matter turnover is governed by accessibility not recalcitrance. *Global Change Biology*, *18*(6), 1781–1796. https://doi.org/10.1111/j.1365-2486.2012.02665.x

Dutta, K., Schuur, E. A. G., Neff, J. C., & Zimov, S. A. (2006). Potential carbon release from permafrost soils of Northeastern Siberia. *Global Change Biology*, *12*(12), 2336–2351. https://doi.org/10.1111/j.1365-2486.2006.01259.x

Dynarski, K. A., Bossio, D. A., & Scow, K. M. (2020). Dynamic stability of soil carbon: Reassessing the "permanence" of soil carbon sequestration. *Frontiers in Environmental Science*, *8*. https://doi.org/10.3389/fenvs.2020.514701

Eliasson, P. E., McMurtrie, R. E., Pepper, D. A., Strömgren, M., Linder, S., & Ågren, G. I. (2005). The response of heterotrophic CO_2 flux to soil warming. *Global Change Biology*, *11*(1), 167–181. https://doi.org/10.1111/j.1365-2486.2004.00878.x

Ellert, B. H., & Bettany, J. R. (1995). Calculation of organic matter and nutrients stored in soils under contrasting management regimes. *Canadian Journal of Soil Science*, *75*(4), 529–538. https://doi.org/10.4141/cjss95-075

Environment Climate Change Canada. (2020). Canadian climate normals 1982-2010 station data. Temperature and Precipitation Graph for 1981 to 2010 Canadian Climate Normals WHITEHORSE A. Government of Canada. https://climate.weather.gc.ca/climate_normals/results_1981_2010_e.html?searchType=stnName&txtStationName=whitehorse&searchMethod=contains&txtCentralLatMin=0&txtCentralLatSec=0&txtCentralLongMin=0&txtCentralLongSec=0&stnID=1617&dispBack=0

FAO; ITPS. (2017). *Global soil organic carbon map – GSOCmap*. Author.

Ferlian, O., Wirth, C., & Eisenhauer, N. (2017). Leaf and root C-to-N ratios are poor predictors of soil microbial biomass C and respiration across 32 tree species. *Pedobiologia*, *65*, 16–23. https://doi.org/10.1016/j.pedobi.2017.06.005

Fierer, N., Schimel, J. P., & Holden, P. A. (2003). Variations in microbial community composition through two soil depth profiles. *Soil Biology and Biogeochemistry*, *35*, 167–176. https://doi.org/10.1016/S0038-0717(02)00251-1

Fraser, T., Colpron, M., & Relf, C. (2018). Evaluating geothermal potential in Yukon through temperature gradient drilling. In K. E. MacFarlane (Eds.), *Yukon exploration and geology* (pp. 75–90). Yukon Geological Survey.

Hassink, J. (1994). Effect of soil texture on the size of the microbial biomass and on the amount of C and N mineralized per unit of microbial biomass in Dutch grassland soils. *Soil Biology and Biochemistry*, *26*(11), 1573–1581. https://doi.org/10.1016/0038-0717(94)90100-7

Heimann, M., & Reichstein, M. (2008). Terrestrial ecosystem carbon dynamics and climate feedbacks. *Nature*, *451*(7176), 289–292. https://doi.org/10.1038/nature06591

Hicks Pries, C. E., Castanha, C., Porras, R. C., & Torn, M. S. (2017). The whole-soil carbon flux in response to warming. *Science*, *355*(6332), 1420–1423. https://doi.org/10.1126/science.aal1319

Ineson, P., Benham, D. G., Poskitt, J., Harrison, A. F., Taylor, K., & Woods, C. (1998). Effects of climate change on nitrogen dynamics in upland soils. 2. A soil warming study. *Global Change Biology*, *4*, 153–161. https://doi.org/10.1046/j.1365-2486.1998.00119.x

IPCC. (2013). In T. F. Stocker, D. Qin, G.-K. Plattner, M. Tignor, S. K. Allen, J. Boschung, A. Nauels, Y. Xia, V. Bex, & P. M. Midgley (Eds.), *Climate change 2013. The physical science basis working group I contribution to the fifth assessment report of the Intergovernmental Panel on Climate Change*. Author.

IPCC. (2019). In H.-O. Pörtner, D. C. Roberts, V. Masson-Delmotte, P. Zhai, M. Tignor, E. Poloczanska, K. Mintenbeck, A. Alegría, M. Nicolai, A. Okem, J. Petzold, B. Rama, & N. W. Weyer (Eds.), *IPCC special report on the ocean and cryosphere in a changing climate*. Author.

International Organization for Standardization. (2005). ISO 10390:2005 Soil quality - Determination of pH.

Karhu, K., Fritze, H., Hämäläinen, K., Vanhala, P., Jungner, H., Oinonen, M., Sonninen, E., Tuomi, M., Spetz, P., Kitunen, V., & Liski, J. (2010). Temperature sensitivity of soil carbon fractions in boreal forest soil. *Ecology*, *91*(2), 370–376. https://doi.org/10.1890/09-0478.1

Kassambra, A. (2020). ggpubr: 'ggplot2' based publication ready plots. Version R package version 0.4.0. https://CRAN.R-project.org/package=ggpubr

Keuskamp, J. A., Dingemans, B. J. J., Lehtinen, T., Sarneel, J. M., & Hefting, M. M. (2013). Tea Bag Index: A novel approach to collect uniform decomposition data across ecosystems. *Methods in Ecology and Evolution*, *4*(11), 1070–1075. https://doi.org/10.1111/2041-210X.12097

Knorr, W., Prentice, I. C., House, J. I., & Holland, E. A. (2005). Long-term sensitivity of soil carbon turnover to warming. *Nature*, *433*, 298–301. https://doi.org/10.1038/nature03226

Koarashi, J., Hockaday, W. C., Masiello, C. A., & Trumbore, S. E. (2012). Dynamics of decadally cycling carbon in subsurface soils. *Journal of Geophysical Research*, *117*(G03033), 1–13. https://doi.org/10.1029/2012JG002034

Kögel-Knabner, I., Guggenberger, G., Kleber, M., Kandeler, E., Kalbitz, K., Scheu, S., Eusterhues, K., & Leinweber, P. (2008). Organo-mineral associations in temperate soils: Integrating biology, mineralogy, and organic matter chemistry. *Journal of Plant Nutrition and Soil Science*, *171*(1), 61–82. https://doi.org/10.1002/jpln.200700048

Köhn, M. (1929). Korngrößenanalyse vermittels Pipettanalyse. *Tonindustrie-Zeitung*, *53*, 729–731.

Lajtha, K., Townsend, K. L., Kramer, M. G., Swanston, C., Bowden, R. D., & Nadelhoffer, K. (2014). Changes to particulate versus mineral-associated soil carbon after 50 years of litter manipulation in forest and prairie experimental ecosystems. *Biogeochemistry*, *119*(1–3), 341–360. https://doi.org/10.1007/s10533-014-9970-5

Langevin, H., Raymond, J., & Fraser, T. (2019). Assessment of thermo-hydraulic properties of rock samples near Takhini Hot Springs, Yukon. In K. E. MacFarlane (Eds.), *Yukon exploration and geology* (pp. 57–73). Yukon Geological Survey.

Larsbo, M., Koestel, J., Kätterer, T., & Jarvis, N. (2016). Preferential transport in macropores is reduced by soil organic carbon. *Vadose Zone Journal*, *15*(9). https://doi.org/10.2136/vzj2016.03.0021

Lavallee, J. M., Soong, J. L., & Cotrufo, M. F. (2019). Conceptualizing soil organic matter into particulate and mineral-associated forms to address global change in the 21st century. *Global Change Biology*, *26*(1), 261–273. https://doi.org/10.1111/gcb.14859

Li, Y., Qing, Y., Lyu, M., Chen, S., Yang, Z., Lin, C., & Yang, Y. (2018). Effects of artificial warming on different soil organic carbon and nitrogen pools in a subtropical plantation. *Soil Biology and Biochemistry*, *124*, 161–167. https://doi.org/10.1016/j.soilbio.2018.06.007

Liebmann, P., Wordell-Dietrich, P., Kalbitz, K., Mikutta, R., Kalks, F., Don, A., Woche, S. K., Dsilva, L. R., & Guggenberger, G. (2020). Relevance of aboveground litter for soil organic matter formation – A soil profile perspective. *Biogeosciences*, *17*(12), 3099–3113. https://doi.org/10.5194/bg-17-3099-2020

Ludwig, M., Achtenhagen, J., Miltner, A., Eckhardt, K.-U., Leinweber, P., Emmerling, C., & Thiele-Bruhn, S. (2015). Microbial contribution to SOM quantity and quality in density fractions of temperate arable soils. *Soil Biology and Biochemistry*, *81*, 311–322. https://doi.org/10.1016/j.soilbio.2014.12.002

Luo, Y., Wan, S., Wallace, D. L. (2001). Acclimatization of soil respiration to warming in a tall grass prairie. *Nature*, *413*, 622–625. https://doi.org/10.1038/35098065

Lützow, M. V., Kögel-Knabner, I., Ekschmitt, K., Flessa, H., Guggenberger, G., Matzner, E., & Marschner, B. (2007). SOM fractionation methods: Relevance to functional pools and to stabilization mechanisms. *Soil Biology and Biochemistry*, *39*(9), 2183–2207. https://doi.org/10.1016/j.soilbio.2007.03.007

Manzoni, S. (2017). Flexible carbon-use efficiency across litter types and during decomposition partly compensates nutrient imbalances-results from analytical stoichiometric models. *Frontiers in Microbiology*, *8*, 661. https://doi.org/10.3389/fmicb.2017.00661

Melillo, J. M., Frey, S. D., DeAngelis, K. M., Werner, W. J., Bernard, M. J., Bowles, F. P., Pold, G., Knorr, M. A., & Grandy, A. S. (2017). Long-term pattern and magnitude of soil carbon feedback to the climate system in a warming world. *Science*, *358*(6359), 101–105. https://doi.org/10.1126/science.aan2874

Melillo, J. M., Steudler, P. A., Aber, J. D., Newkirk, K., Lux, H., Bowles, F. P., Catricala, C., Magill, A., Ahrens, T., & Morrisseau, S. (2002). Soil warming and carbon-cycle feedbacks to the climate system. *Science*, *298*(5601), 2173–2176. https://doi.org/10.1126/science.1074153

Mougeot, C. M. (1997). Soil, Terrain and Wetland survey of the city of Whitehorse. Draft Report with maps at 1:20000 scale. Mougeot Geoanalysis. Whitehorse.

Nieder, R., Benbi, D. K., & Scherer, H. W. (2011). Fixation and defixation of ammonium in soils: A review. *Biology and Fertility of Soils*, *47*(1), 1–14. https://doi.org/10.1007/s00374-010-0506-4

Nottingham, A. T., Meir, P., Velasquez, E., & Turner, B. L. (2020). Soil carbon loss by experimental warming in a tropical forest. *Nature*, *584*(7820), 234–237. https://doi.org/10.1038/s41586-020-2566-4

Ofiti, N. O. E., Zosso, C. U., Soong, J. L., Solly, E. F., Torn, M. S., Wiesenberg, G. L. B., & Schmidt, M. W. I. (2021). Warming promotes loss of subsoil carbon through accelerated degradation of plant-derived organic matter. *Soil Biology and Biochemistry*, *156*, 108185. https://doi.org/10.1016/j.soilbio.2021.108185

O'Gorman, E. J., Benstead, J. P., Cross, W. F., Friberg, N., Hood, J. M., Johnson, P. W., Sigurdsson, B. D., & Woodward, G. (2014). Climate change and geothermal ecosystems: Natural laboratories, sentinel systems, and future refugia. *Global Change Biology*, *20*(11), 3291–3299. https://doi.org/10.1111/gcb.12602

Oksanen, J., Blanchet, F. G., Friendly, M., Kindt, R., Legendre, P., McGlinn, D., Minchin, P. R., O'Hara, R. B., Simpson, G. L., Solymos, P., Stevens, M. H. H., Szoecs, E., & Wagner, H. (2019). Community ecology package 'vegan'. Version 2.5-6. https://cran.r-project.org, https://github.com/vegandevs/vegan

Pacific Climate Impacts Consortium (PCIC). (2014). *Statistically downscales climate scenarios*. University of Victoria. https://www.pacificclimate.org/data/statistically-downscaled-climate-scenarios

Pearson, R. K., Neuvo, Y., Astola, J., & Gabbouj, M. (2016). Generalized hampel filters. *EURASIP Journal on Advances in Signal Processing*, *2016*(1), https://doi.org/10.1186/s13634-016-0383-6

Poeplau, C., & Don, A. (2013). Sensitivity of soil organic carbon stocks and fractions to different land-use changes across Europe. *Geoderma*, *192*, 189–201. https://doi.org/10.1016/j.geoderma.2012.08.003

Poeplau, C., Don, A., Six, J., Kaiser, M., Benbi, D., Chenu, C., Cotrufo, M. F., Derrien, D., Gioacchini, P., Grand, S., Gregorich, E., Griepentrog, M., Gunina, A., Haddix, M., Kuzyakov, Y., Kühnel, A., Macdonald, L. M., Soong, J., Trigalet, S., … Nieder, R. (2018). Isolating organic carbon fractions with varying turnover rates in temperate agricultural soils – A comprehensive method comparison. *Soil Biology and Biochemistry*, *125*, 10–26. https://doi.org/10.1016/j.soilbio.2018.06.025

Poeplau, C., Don, A., Vesterdal, L., Leifeld, J., Van wesemael, B., Schumacher, J., & Gensior, A. (2011). Temporal dynamics of soil organic carbon after land-use change in the temperate zone – Carbon response functions as a model approach. *Global Change Biology*, *17*(7), 2415–2427. https://doi.org/10.1111/j.1365-2486.2011.02408.x

Poeplau, C., Kätterer, T., Leblans, N. I. W., & Sigurdsson, B. D. (2016). Sensitivity of soil carbon fractions and their specific stabilization mechanisms to extreme soil warming in a subarctic grassland. *Global Change Biology*, *23*(3), 1316–1327. https://doi.org/10.1111/gcb.13491

Poeplau, C., Sigurðsson, P., & Sigurdsson, B. D. (2020). Depletion of soil carbon and aggregation after strong warming of a subarctic Andosol under forest and grassland cover. *SOIL*, *6*(1), 115–129. https://doi.org/10.5194/soil-6-115-2020

Poeplau, C., Vos, C., & Don, A. (2017). Soil organic carbon stocks are systematically overestimated by misuse of the parameters bulk density and rock fragment content. *SOIL*, *3*(1), 61–66. https://doi.org/10.5194/soil-3-61-2017

R Core Team. (2019). *R: A language and environment for statistical computing*. Version 3.6.1. R Foundation for Statistical Computing. https://www.R-project.org/

Rumpel, C., & Kögel-Knabner, I. (2011). Deep soil organic matter—A key but poorly understood component of terrestrial C cycle. *Plant and Soil*, *338*(1–2), 143–158. https://doi.org/10.1007/s11104-010-0391-5

Rustad, L., Campbell, J., Marion, G., Norby, R., Mitchell, M., Hartley, A., Cornelissen, J., & Gurevitch, J. (2001). A meta-analysis of the response of soil respiration, net nitrogen mineralization, and

aboveground plant growth to experimental ecosystem warming. *Oecologia*, *126*(4), 543–562. https://doi.org/10.1007/s004420000544

Schauberger, P., & Walker, A. (2020). openxlsx: Read, write and edit xlsx files. Version R package version 4.2.3. https://CRAN.R-project.org/package=openxlsx

Schöning, I., Totsche, K. U., & Kögel-Knabner, I. (2006). Small scale variability of organic carbon stocks in litter and solum of a forested Luvisol. *Geoderma*, *136*(3–4), 631–642. https://doi.org/10.1016/j.geoderma.2006.04.023

Shi, Z., Allison, S. D., He, Y., Levine, P. A., Hoyt, A. M., Beem-Miller, J., Zhu, Q., Wieder, W. R., Trumbore, S., & Randerson, J. T. (2020). The age distribution of global soil carbon inferred from radiocarbon measurements. *Nature Geoscience*, *6*, 555–559. https://doi.org/10.1038/s41561-020-0596-z

Sigurdsson, B. D., Leblans, N. I. W., Dauwe, S., Guðmundsdóttir, E., Gundersen, P., Gunnarsdóttir, G. E., Holmstrup, M., Ilieva-Makulec, K., Kätterer, T., Marteinsdóttir, B., Maljanen, M., Oddsdóttir, E. S., Ostonen, I., Peñuelas, J., Poeplau, C., Richter, A., Sigurðsson, P., van Bodegom, P., Wallander, H., … Janssens, I. (2016). Geothermal ecosystems as natural climate change experiments: The ForHot research site in Iceland as a case study. *Icelandic Agricultural Sciences*, *29*, 53–71. https://doi.org/10.16886/ias.2016.05

Smith, C. A. S., Burn, C. R., Tarnocai, C., & Sproule, B. (1998). Air and soil temperature relations along an ecological transect through the permafrost zones of northwestern Canada. In: PERMAFROST - Seventh International Conference (Proceedings), Yellowknife (Canada), Collection Nordicana, *55*, 1009–1015.

Smith, C. A. S., Roots, C. F., & Roots, M. (Eds.). (2004). *Ecoregions of the Yukon Territory; biophysical properties of Yukon landscapes*. PARC Technical Bulletin 04-01.

Sokol, N. W., Sanderman, J., & Bradford, M. A. (2019). Pathways of mineral-associated soil organic matter formation: Integrating the role of plant carbon source, chemistry, and point of entry. *Global Change Biology*, *25*(1), 12–24. https://doi.org/10.1111/gcb.14482

Song, J., Wan, S., Piao, S., Knapp, A. K., Classen, A. T., Vicca, S., Ciais, P., Hovenden, M. J., Leuzinger, S., Beier, C., Kardol, P., Xia, J., Liu, Q., Ru, J., Zhou, Z., Luo, Y., Guo, D., Adam Langley, J., Zscheischler, J., … Zheng, M. (2019). A meta-analysis of 1,119 manipulative experiments on terrestrial carbon-cycling responses to global change. *Nature Ecology & Evolution*, *3*(9), 1309–1320. https://doi.org/10.1038/s41559-019-0958-3

Takriti, M., Wild, B., Schnecker, J., Mooshammer, M., Knoltsch, A., Lashchinskiy, N., Alves, R. J. E., Gentsch, N., Gittel, A., Mikutta, R., Wanek, W., & Richter, A. (2018). Soil organic matter quality exerts a stronger control than stoichiometry on microbial substrate use efficiency along a latitudinal transect. *Soil Biology and Biochemistry*, *121*, 212–220. https://doi.org/10.1016/j.soilbio.2018.02.022

van Gestel, N., Shi, Z., van Groenigen, K. J., Osenberg, C. W., Andresen, L. C., Dukes, J. S., Hovenden, M. J., Luo, Y., Michelsen, A., Pendall, E., Reich, P. B., Schuur, E. A. G., & Hungate, B. A. (2018). Predicting soil carbon loss with warming. *Nature*, *554*(7693), E4–E5. https://doi.org/10.1038/nature25745

Walker, T. W. N., Janssens, I. A., Weedon, J. T., Sigurdsson, B. D., Richter, A., Peñuelas, J., Leblans, N. I. W., Bahn, M., Bartrons, M., De Jonge, C., Fuchslueger, L., Gargallo-Garriga, A., Gunnarsdóttir, G. E., Marañón-Jiménez, S., Oddsdóttir, E. S., Ostonen, I., Poeplau, C., Prommer, J., Radujković, D., … Verbruggen, E. (2020). A systemic overreaction to years versus decades of warming in a subarctic grassland ecosystem. *Nature Ecology & Evolution*, *4*, 101–108. https://doi.org/10.1038/s41559-019-1055-3

Walker, T. W. N., Kaiser, C., Strasser, F., Herbold, C. W., Leblans, N. I. W., Woebken, D., Janssens, I. A., Sigurdsson, B. D., & Richter, A. (2018). Microbial temperature sensitivity and biomass change explain soil carbon loss with warming. *Nature Climate Change*, *8*(10), 885–889. https://doi.org/10.1038/s41558-018-0259-x

Wickham, H. (2007). Reshaping data with the reshape package. *Journal of Statistical Software*, *21*, 1–20. http://www.jstatsoft.org/v21/i12/

Wickham, H. (2011). The split-apply-combine strategy for data analysis. *Journal of Statistical Software*, *40*(1), 1–29. https://doi.org/10.18637/jss.v040.i01

Wickham, H. (2016). *ggplot2: Elegant graphics for data analysis*. Springer-Verlag. https://ggplot2.tidyverse.org

Wickham, H., & Bryan, J. (2019). readxl: Read excel files. Version R package version 1.3.1. https://CRAN.R-project.org/package=readxl

Wickham, H., François, R., Henry, L., & Müller, K. (2020). dplyr: A grammar of data manipulation. Version R package version 1.0.0.r. https://CRAN.R-project.org/package=dplyr

Wordell-Dietrich, P., Don, A., & Helfrich, M. (2017). Controlling factors for the stability of subsoil carbon in a Dystric Cambisol. *Geoderma*, *304*, 40–48. https://doi.org/10.1016/j.geoderma.2016.08.023

Zimmermann, M., Leifeld, J., Schmidt, M. W. I., Smith, P., & Fuhrer, J. (2007). Measured soil organic matter fractions can be related to pools in the RothC model. *European Journal of Soil Science*, *58*(3), 658–667. https://doi.org/10.1111/j.1365-2389.2006.00855.x

SUPPORTING INFORMATION

Additional supporting information may be found online in the Supporting Information section.

How to cite this article: Peplau, T., Schroeder, J., Gregorich, E., & Poeplau, C. (2021). Long-term geothermal warming reduced stocks of carbon but not nitrogen in a subarctic forest soil. *Global Change Biology*, 27, 5341–5355. https://doi.org/10.1111/gcb.15754